

QCD analysis of the CMS inclusive differential Z production data at $\sqrt{s} = 8$ TeV

Rajdeep M. Chatterjee,¹ Monoranjan Guchait,¹ and Ringailė Plačakytė²¹*Department of High Energy Physics, Tata Institute of Fundamental Research Homi Bhabha Road, Mumbai 400005, India*²*Deutsches Elektronen-Synchrotron DESY Notkestraße 85, D-22607 Hamburg, Germany*
(Received 17 June 2016; published 23 August 2016)

The parton distribution functions (PDFs) of the proton are one of the essential ingredients to describe physics processes at hadron colliders. The Z boson production data at the LHC have a potential to constrain PDFs, especially the gluon distribution. In this study the CMS measurement of the inclusive double differential Z boson production cross section in terms of transverse momentum and rapidity is compared to the next-to-leading order theory predictions at the center-of-mass energy, $\sqrt{s} = 8$ TeV with an integrated luminosity of 19.71 fb^{-1} . In addition, the sensitivity of this measurement to PDFs is studied within the framework of the HERAFitter. A moderate improvement to the gluon distribution is observed at the Bjorken $x \approx 0.1$ region. However, in order to obtain further improvement to the gluon distribution in the global fits, the higher-order theory calculations accessible via fast techniques are necessary.

DOI: [10.1103/PhysRevD.94.034035](https://doi.org/10.1103/PhysRevD.94.034035)

I. INTRODUCTION

The precision measurements of the Standard Model (SM) of particle physics are one of the top priority programs at the LHC. The accurate theory predictions are necessary in order to completely exploit the potential of the SM measurements. Importantly, in the hadron colliders parton distribution functions (PDFs) are one of the necessary ingredients for theory predictions. Naively, the PDF $f_i(x, Q^2)$ represents the probability of finding a parton of flavor i [where $i: g$ (gluons), q (quarks); $q = u, d, c, s, \dots$] inside a proton carrying a fraction x of the momentum of the proton at the scale Q , called the factorization scale, related to the hard scale of the involved physical process. The PDFs cannot be derived from the first principles of quantum chromodynamics (QCD) [1] and have to be constrained experimentally. The PDFs are constrained primarily by the deep inelastic scattering (DIS) data. Additional constraints come from the fixed-target, Tevatron and LHC measurements (for more details, see, for example, the reviews in Refs. [2,3] and references therein).

Currently, various published SM measurements at the LHC with the center-of-mass energies 7 and 8 TeV are already used in the global PDF fits [4–7]. Besides these global PDF fitting efforts, the sensitivity of the particular LHC measurement to PDFs is also studied. For example, PDFs are constrained using the measurement of the W and Z production to strange quark distribution in ATLAS [8], the CMS W charge asymmetry [9] and W in association with the charm quark measurements at 7 TeV [10], W boson production in association with a single charm quark in ATLAS [11], the inclusive jet cross sections from the LHC [12–15], top quark pair production [16,17], etc. In this

current analysis, the impact on the PDFs of the CMS production cross section measurement of the Z boson decaying to a pair of muons [18,19] is studied. This measurement is performed in various bins of transverse momentum [$p_T(Z)$] and rapidity [$Y(Z)$] of the Z boson. The QCD analysis is performed at the next-to-leading order (NLO) in the framework of the HERAFitter [20]. Along with the CMS Z boson measurements, the inclusive HERA-I DIS [21] and the CMS W muon asymmetry data [9] are used in this study.

This paper is organized as follows. In Sec. II we discuss the inclusive Z boson production at the LHC, while in Sec. III the correlation studies of the different partons with the Z boson production are presented. The general settings of the QCD analysis and the results are presented in Secs. IV and V, respectively, followed by a summary in Sec. VI.

II. INCLUSIVE Z PRODUCTION AT THE LHC

At the LHC experiment, the Z boson production cross section is one of the high priority measurements to understand the detector performance as well as for precision tests of the SM. The inclusive Z boson production at the LHC is initiated by the subprocesses,

$$q\bar{q}, \quad gq \rightarrow Z + n\text{jets}, \quad (1)$$

at LO, where $n \geq 0$. At the low $p_T(Z)$ region, $p_T(Z) \lesssim 20 \text{ GeV}$, the subprocess with initial state $q\bar{q}$ has significant contribution to the total cross section, while in the high $p_T(Z)$ region, $p_T(Z) \lesssim M_Z/2$, the subprocess gq becomes dominant ($\sim 70\%$ – 80%). These relative subprocess contributions are also valid at the NLO accuracy

[12,22,23]. Therefore, the inclusive Z boson production cross section is one of the potential measurements to probe the gluon density inside the proton at the LHC [24].

The vector boson (W , Z) production in hadron colliders has a very rich physics potential and is well studied in the literature [25–27]. Currently, the inclusive Z boson production in its leptonic decay channel is computed at the next-to-next-to-leading order (NNLO) level [$\mathcal{O}(\alpha_s^2)$] by several groups [28,29], and the K -factor which is defined to be the ratio of the NNLO and LO cross sections, is estimated to be about ~ 1.4 – 1.6 depending on the kinematic phase space. These NNLO predictions are equivalent to NLO for the $Z + n$ -jet ($n \geq 1$) process which is of the same order [$\mathcal{O}(\alpha_s^2)$]. It is to be noted that these NLO predictions work quite well for the high $p_T(Z)$ regime. However, for the low $p_T(Z)$ range where the soft gluon emission with very low transverse momentum takes place, the NLO predictions may become unstable. In this low $p_T(Z)$ region, the fixed order perturbative calculation fails due to the presence of large logarithmic terms $\sim \log(M_Z/p_T)$. Therefore, in order to make the calculation realistic at this low transverse momentum region, the large logarithms must be resummed to all orders of α_s . In Refs. [30,31] the soft gluon nonperturbative effects are taken into account by resumming all logarithm terms in the Z boson production, and it can be computed using the software package ResBos.

The full NNLO QCD corrections [$\mathcal{O}(\alpha_s^2)$] to the $p_T(Z)$ and $p_T(W)$ distributions in association with jets became available very recently [32–35]. However, before that, an attempt has been made to compute the two-loop QCD corrections to the process $gg \rightarrow Zj$ using the helicity amplitudes [36] method.

At the LHC, both the CMS and the ATLAS Collaborations have measured the inclusive Z boson production cross section in proton-proton collisions at the center-of-mass energies of $\sqrt{s} = 7$ [37] and 8 TeV [19]. These measurements are performed by identifying the Z boson in both the electron and muon channels, and the results are presented in terms of the differential distributions of the Z boson. In particular, the CMS measurements relevant in the present context, the differential cross sections, are obtained in terms of the $p_T(Z)$ and absolute $Y(Z)$ of the Z boson [18,19] based on the data sample of pp collisions at $\sqrt{s} = 8$ TeV corresponding to an integrated luminosity of 19.71 fb^{-1} . The results are presented in five absolute rapidity bins ranging from 0 to 2.0, and the entire $p_T(Z)$ range has been divided into 10 bins reaching up to 1 TeV. The main goal of this current study is to test the sensitivity of the high $p_T(Z)$ data to the gluon PDF: hence, the measurements of the first two bins (0–20 GeV and 20–40 GeV) are not included in the QCD analysis. The various sources of uncertainties related to the measurement techniques and the background estimation are obtained with the bin-to-bin correlation for each uncertainty source and

accounted for in terms of covariance matrices. It is observed that the luminosity measurement is a main source of uncertainty amounting to 2.6%, leading to a total uncertainty of $\sim 3\%$ – 4% in the measurement [18,19]. It is important to note that in this measurement, no selection has been made on jets accompanied by the Z boson in order to avoid a possibly sizable (5%–10%) contribution to the total systematic uncertainties from jet energy scale measurements. The measured cross sections are presented by unfolding the detector effects at the parton level to be compared with higher order theory predictions. In Ref. [19], a comparison of data to the theoretical predictions from the FEWZ computation [38] for all rapidity bins is presented. The level of agreement between the data and the theoretical prediction is found to be of $\mathcal{O}(\sim 10\%)$ across all $p_T(Z)$ and $Y(Z)$ bins, which is within the uncertainties of the measurement and the theoretical prediction. The uncertainty in the theoretical predictions includes the variation of the QCD scales and PDF.

In the present QCD analysis, the inclusive Z boson differential cross sections are calculated at NLO using the MCFM [39] interfaced to AppGrid [40]. The transverse momenta of the leading (subleading) muons are required to be greater than 25(10) GeV and less than 2.4(2.1) in absolute rapidity, whereas the dimuon invariant mass is selected to be within 81–101 GeV. The NLO CT10 PDF set [41] is used for the Z -boson event generation and the factorization (μ_F), and the renormalization (μ_R) scales are set to the dynamical scale $\mu_0 = \sqrt{(p_T(Z))^2 + M_Z^2}$. The uncertainties in the $p_T(Z)$ distribution due to the choices of QCD scales and PDF are also computed. The uncertainty due to the QCD scales is obtained by varying the scales, $\mu_R, \mu_F = \{1/2, 2\} \times \mu_0$. It is observed that the QCD scale uncertainty is about 5% at the low $p_T(Z)$ region and rises to $\sim 7\%$ at the high $p_T(Z)$ region. The PDF uncertainty is derived following the asymmetric uncertainty prescription [42] by generating the $p_T(Z)$ spectrum for all the up- and down-type eigenvectors of the NNPDF2.3 [43] PDF set and found to be about 2%–3%. Evidently, the scale uncertainty dominates over the other theoretical uncertainties.

The comparison between the MCFM theory predictions and the measured double differential Z boson cross section normalized to the inclusive cross section for various $p_T(Z)$ and $Y(Z)$ bins corresponding to an integrated luminosity of 19.71 fb^{-1} is presented in Fig. 1. In addition, the ratios of the data and the theory predictions are also presented along with the PDF and QCD scale uncertainty band. As can be seen in Fig. 1, a disagreement of about 10% exists between the measured cross section and the MCFM theory prediction across all the rapidity bins except for the last bin [$1.6 < Y(Z) < 2.0$] where the discrepancy is even larger. Note that a similar level of agreement of the inclusive Z boson data is also observed with the theory predictions provided by FEWZ [19]. Recently, in Ref. [44], the ATLAS

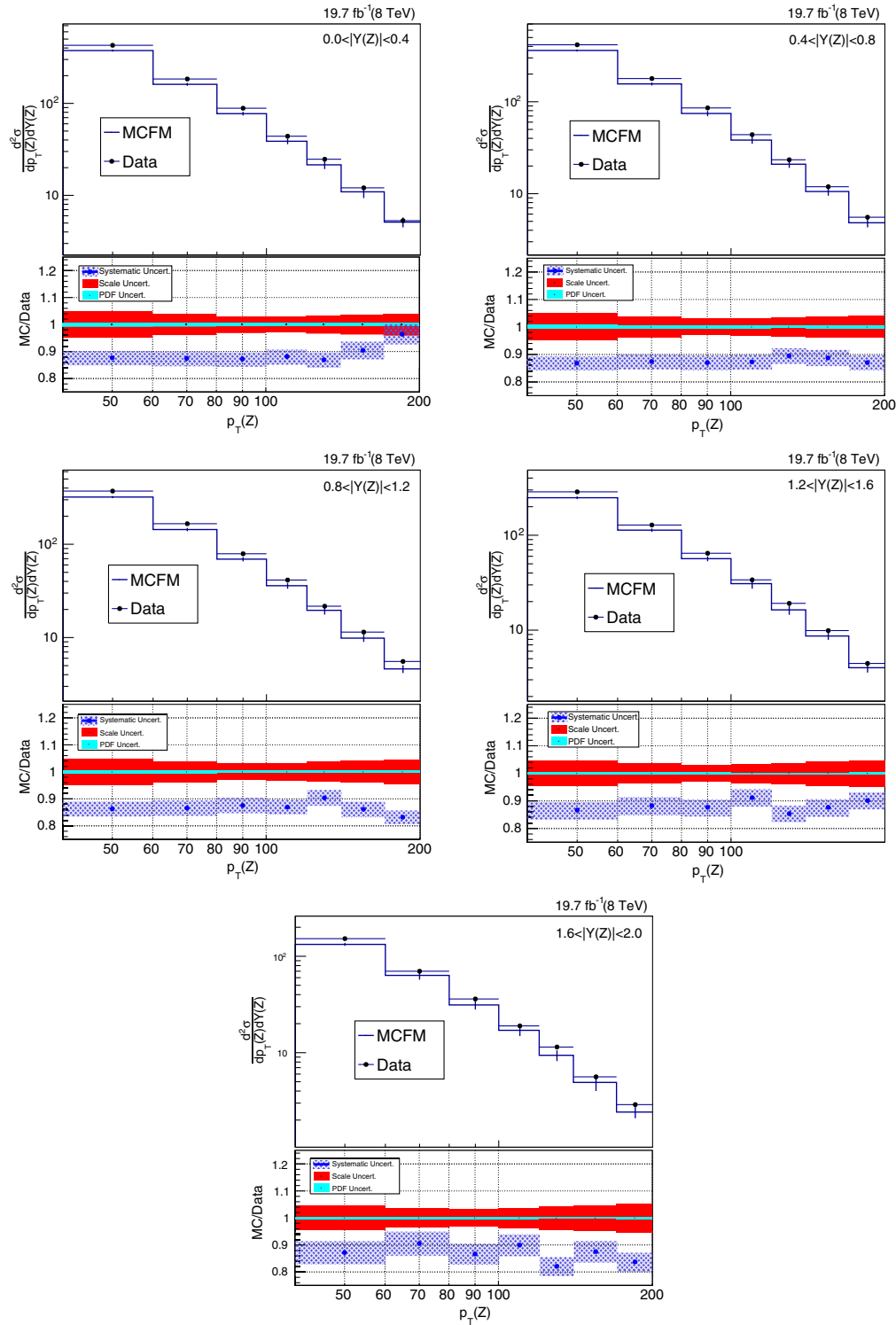


FIG. 1. The comparison of Z boson CMS data to the theory predictions obtained from the MCFM [39] in different Z rapidity [Y(Z)] bins.

and CMS data at 7 TeV for V + jet (V = W, Z) processes are compared with NNLO theory predictions.

III. PARTON CORRELATION

In order to understand the sensitivity of the initial PDFs to the Z boson production cross

section, the correlation of the corresponding PDFs with the cross section is studied using the NNPDF2.3 [43] PDF set. The correlation function, Q_i for each *i*th parton (*i* = *g*, *u*, *d*, *s*), is computed by evaluating means and standard deviations from the set of N_{rep} as

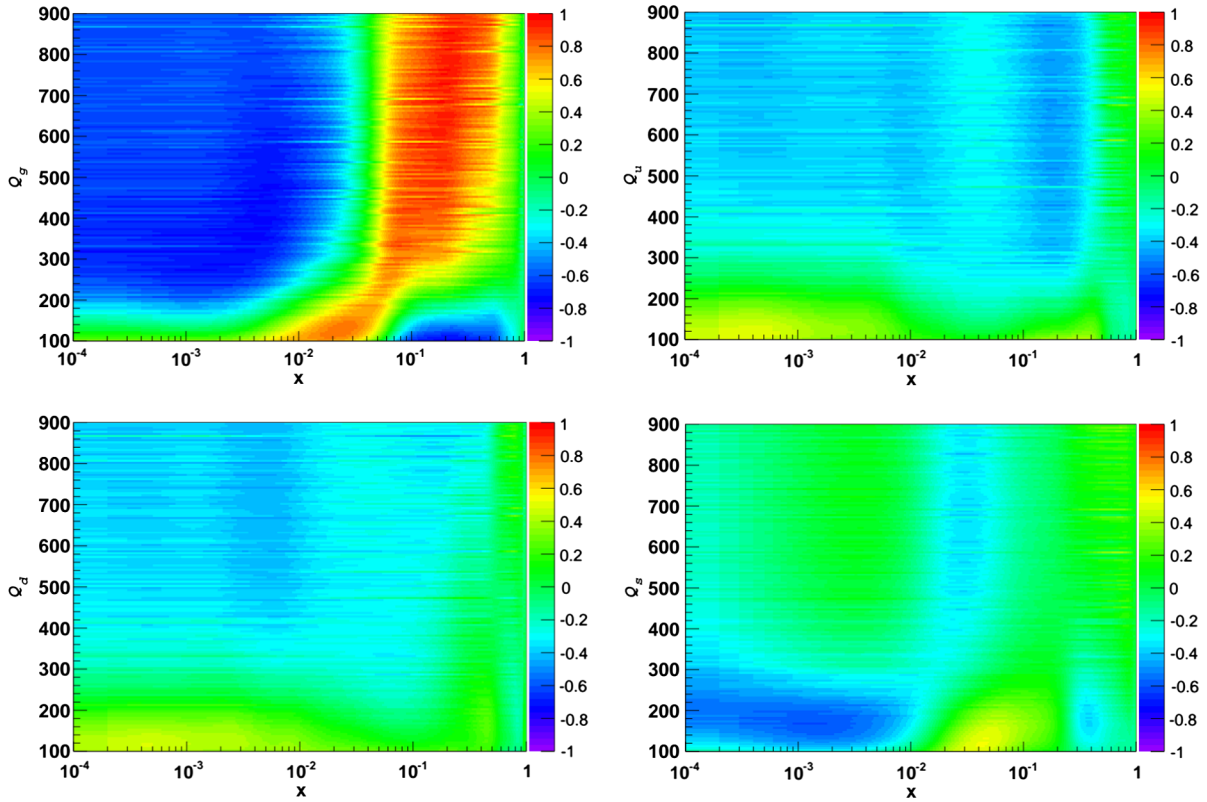


FIG. 2. Correlation coefficients (Q_i ; $i = g, u, d, s$) between the gluon (top left), the up quark (top right), the down quark (bottom left) and the strange quark (bottom right) PDFs and the inclusive Z boson production cross section for the $p_T(Z) > 40$ GeV range.

$$Q_i[\sigma_{\text{incl}}, x f_i(x, \mu^2)] = \frac{N_{\text{rep}}}{N_{\text{rep}} - 1} \mathcal{F}_i(\sigma_{\text{incl}}, x, \mu^2)$$

where

$$\mathcal{F}_i(\sigma_{\text{incl}}, x, \mu^2) = \frac{\langle \sigma_{\text{incl}} x f_i(x, \mu^2) \rangle - \langle \sigma_{\text{incl}} \rangle \langle x f_i(x, \mu^2) \rangle}{\Delta_{\sigma_{\text{incl}}} \Delta_{x f_i(x, \mu^2)}}, \quad (2)$$

where N_{rep} is the number of replicas in the NNPDF sets, σ_{incl} is the inclusive Z boson production cross section computed using MCFM and $f_i(x, \mu^2)$ is the PDF for a given parton i and the factorization scale μ^2 . In the denominator, the $\Delta_{\sigma_{\text{incl}}}$ and $\Delta_{x f_i(x, \mu^2)}$ are the standard deviations of cross sections for N_{rep} replicas of PDF sets and the PDF replicas themselves, respectively.

Figure 2 presents the correlation coefficients (Q_i) for the gluon, up, down and strange quark PDFs in the x - Q_i plane. The correlation coefficient Q_i close to zero indicates that there is no correlation at all between the respective incoming parton and the production cross section. Similarly, higher values of Q_i indicate the presence of a strong correlation of the corresponding parton and cross sections, whereas negative values mean anticorrelation. The figure representing the gluon correlation (upper left panel) indicates that the inclusive Z boson cross section is strongly sensitive to gluon PDFs for the values of $x \sim 0.01$ – 0.1 .

IV. QCD ANALYSIS

The NLO QCD analysis is performed using the framework of the open source code `HERAFitter (v1.1.0)`, the detailed description of which can be found in Ref. [20]. In this analysis, the initial parametrization for the PDFs is assumed at the starting scale of $Q_0^2 = 1.9$ GeV² and evolved to higher scales with the DGLAP [45–48] equations using `QCDNUM` [49]. The combined data sets from the DIS neutral current (NC) and the charged current (CC) in e^+p and e^-p scattering at the H1 and ZEUS experiments, as well as the CMS W muon charge asymmetry data, are used in this study along with the data corresponding to the measurement of inclusive Z production, as described

TABLE I. Maximum and minimum values of model parameters along with the nominal value for the central fit.

Parameters	Nominal value	Lower limit	Upper limit
f_s	0.31	0.23	0.38
m_c [GeV]	1.4	$1.35(Q_0^2 = 1.8)$	1.65
m_b [GeV]	4.75	4.3	5.0
Q_{min}^2 [GeV ²]	3.5	2.5	5.0
Q_0^2 [GeV ²]	1.9	$1.5(f_s = 0.29)$	$2.5(f_s = 0.34, m_c = 1.6 \text{ GeV})$

TABLE II. Partial χ^2 per data point and global χ^2 per degrees of freedom (dof) for the data sets used in 14-parameter fitting.

Data sets	HERA I	HERA I + CMS (Asym)	HERA I + CMS full
NC HERA H1-ZEUS e^+p	109/145	109/145	109/145
NC HERA H1-ZEUS e^-p	400/379	401/379	411/379
CC HERA H1-ZEUS e^+p	19/34	19/34	19/34
CC HERA H1-ZEUS e^-p	27/34	30/34	31/34
CMS W electron asymmetry	–	8.4/11	7.5/11
CMS W muon asymmetry	–	13/11	13/11
CMS Inclusive Z data	–	–	78.5/40
Total χ^2/dof	555/578	580/600	668/640
$\chi^2 p$ value	0.74	0.71	0.21

above. In order to exploit the precise CMS lepton charge asymmetry data that are used to improve the constraints of the PDFs of light quarks [9], the CMS measurement of W charge asymmetry is added as an additional input along with the inclusive $p_T(Z)$ data.

At the starting scale Q_0^2 , the PDFs are parametrized using a generic form:

$$xf(x) = Ax^B(1-x)^C(1+Dx+Ex^2), \quad (3)$$

Here, A is the normalization term, and the behavior of the PDFs for low (high) values of Bjorken x is regulated by the B (C) term. The optimal parametrization for the PDF fit is found through a parametrization scan as described in [21]: In the beginning, the scan is performed starting from a parametrization with a basic polynomial form, and then additional parameters are allowed to vary, one parameter at a time. This scanning process continues till the reduction in χ^2 reaches a value less than unity.

The final parametrized form with 14 free parameters for the five PDFs, valence light quarks $xu_v(x)$, $xd_v(x)$, the antiquark $x\bar{U}(x)$, $x\bar{D}(x)$, where $x\bar{U}(x) = x\bar{u}(x)$, $x\bar{D}(x) = x\bar{d}(x) + x\bar{s}(x)$, and the gluon $xg(x)$ is defined as

$$\begin{aligned} xg(x) &= A_g x^{B_g} (1-x)^{C_g} + A'_g x^{B'_g} (1-x)^{C'_g}, \\ xu_v(x) &= A_{u_v} x^{B_{u_v}} (1-x)^{C_{u_v}} (1 + E_{u_v} x^2), \\ xd_v(x) &= A_{d_v} x^{B_{d_v}} (1-x)^{C_{d_v}}, \\ x\bar{U}(x) &= A_{\bar{U}} x^{B_{\bar{U}}} (1-x)^{C_{\bar{U}}}, \\ x\bar{D}(x) &= A_{\bar{D}} x^{B_{\bar{D}}} (1-x)^{C_{\bar{D}}}, \end{aligned} \quad (4)$$

The normalization parameters A_{u_v} , A_{d_v} and A_g are constrained by the QCD sum rules. A more expanded form for $g(x)$ is used with the choice $C'_g = 25$ following the approach of the MSTW group [50]. The strange quark relation to \bar{D} is defined as

$$x\bar{s} = f_s x\bar{D}, \quad (5)$$

where f_s is the fraction of strange quarks, $f_s = \frac{\bar{s}}{d+\bar{s}} = 0.31 \pm 0.08$ [2]. Additional constraints applied are $B_{\bar{U}} = B_{\bar{D}}$ and $A_{\bar{U}} = A_{\bar{D}}(1 - f_s)$.

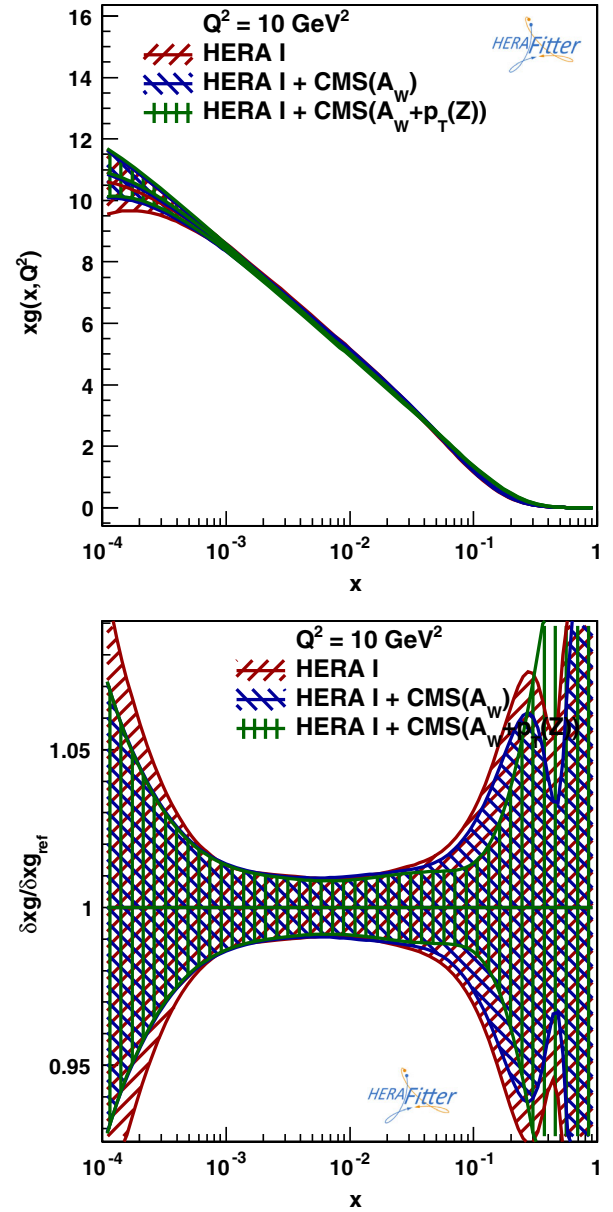
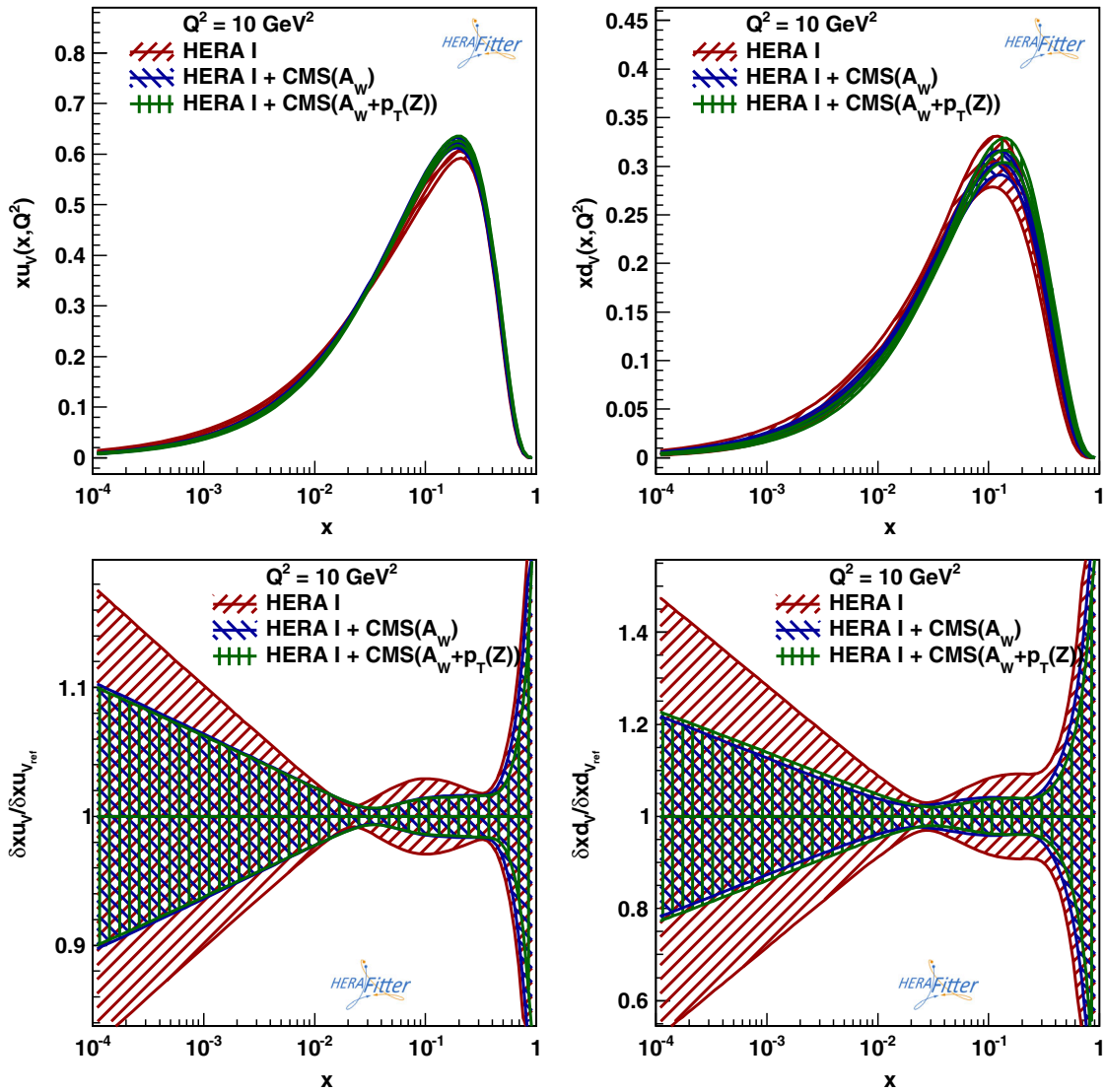


FIG. 3. Distribution of the gluon for $Q^2 = 10 \text{ GeV}^2$. The bands correspond to experimental PDF uncertainties of the fit to HERA data only (red) and both HERA and the CMS data (blue and green).


 FIG. 4. Same as in Fig. 3, but for u (left) and d (right) valence quarks.

The sources of experimental uncertainties in the measurement of the Z boson cross section are discussed in detail in Ref. [19] and taken into account in the fit through a covariance matrix. The uncertainty due to the choice of parametrization given by Eq. (4) is evaluated by assuming an alternate parametrization. The parametrization uncertainties are estimated by including additional terms one by one in the polynomial expansion of Eq. (3) for all parton densities following the procedure described in Ref. [21]. The variation in the starting scale Q_0^2 is regarded as a parametrization uncertainty and is estimated by varying it within the range $1.5(f_s = 0.29) \geq Q_0^2 \geq 2.5(f_s = 0.34, m_c = 1.6)$. The parametrization uncertainty is constructed as an envelope built from the maximal differences between the PDFs. The model uncertainties in the QCD fit are evaluated by varying heavy quark masses m_c and m_b , strange quark fraction parameter f_s , and Q_{\min}^2 . In order to obtain these uncertainties, the model parameters are varied between the maximum

and minimum values one at a time in the fit. The change of the fit due to this variation with respect to the central fit obtained using the nominal value of that parameter is estimated to be the uncertainty corresponding to that model parameter. The model uncertainties with variations are presented in Table I. The experimental, model and parametrization uncertainties are added in quadrature to obtain the total systematic uncertainty.

V. RESULTS

The QCD analysis results are presented in Table II. The quality of the fit is found to be fairly good for the HERA-I data only and HERA-I with CMS W charge asymmetry data. The combined fit of HERA-I data with CMS W and Z production data is observed to be higher due to the fact that the disagreement between the Z boson data and the corresponding MCFM theory prediction is

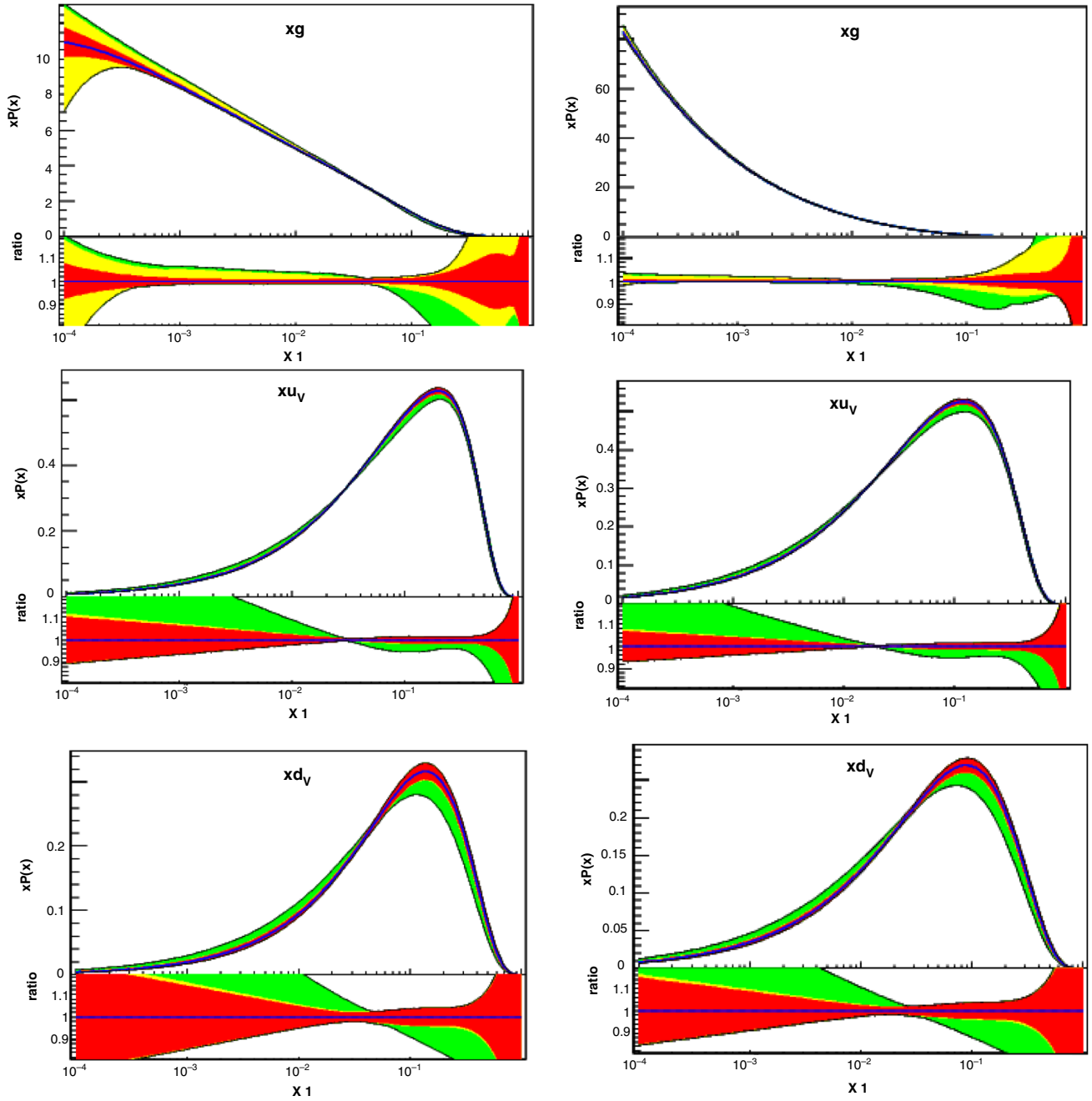


FIG. 5. Constrained parton density functions for the gluon (top), and u (middle) and d valence (bottom) quarks from the QCD analysis of CMS Z boson data at the scales $Q^2 = 10 \text{ GeV}^2$ (left panel) and M_Z^2 (right panel). The uncertainties include those due to the experimental (red), the model (yellow) and the parametrization variations (green). All uncertainties are added in quadrature.

relatively large. However, the total χ^2/dof is found to be reasonable.

The impact of the CMS data to PDFs is illustrated by comparing the PDF fits with the HERA DIS data alone as shown for the gluon in Fig. 3 and for u and d valence quarks in Fig. 4. In order to understand the improvement in gluon distribution due to the addition of the CMS data, the ratio of the relative uncertainties of the fitted gluon distribution obtained using the combined data sets and the DIS data only is presented in the same figure in the bottom panel. A change

of shape of the gluon distribution due to the inclusion of the CMS Z boson data is visible at low x , in particular, around the value of $x \sim 0.1$ where a strong correlation of the gluon PDF with the Z boson production cross section is observed, as shown in Fig. 2. In addition, Fig. 4 shows that the CMS W charge asymmetry is more sensitive to the light quark distributions. The constrained NLO distributions of the gluon, and u and d valence quarks are shown in Fig. 5 for two values of $Q^2 = 10 \text{ GeV}^2$ and M_Z^2 . In general, as observed, the uncertainty due to the parametrization is the dominant one.

VI. SUMMARY

The sensitivity of the CMS Z boson production measurement to PDFs at $\sqrt{s} = 8$ TeV is reported in this paper. The theory predictions corresponding to the CMS Z boson production measurement are obtained from the MCFM-based calculations at NLO. The studies of the initial parton correlations with the Z boson cross section indicate the sensitivity of the gluon distribution in this process. A comparison between the measured Z boson cross section in various $p_T(Z)$ and $Y(Z)$ bins and the corresponding MCFM-based theory predictions at NLO shows an agreement at the level of $\sim 10\%$; however, the shapes of the distributions of both the data and the theory agree reasonably well. A similar level of agreement is also observed by the calculations performed with FEWZ. As evaluated with the MCFM-based theory predictions, the uncertainty due to the QCD scales is found to be the most dominant, of the

order of 5%–7%. It is to be noted that the inclusive double differential Z boson cross section is measured with an overall precision of about 3%–4%, which is remarkably precise for any measurement at the hadron colliders.

The NLO QCD analysis is performed within the framework of the HERAFitter, fitting the CMS Z boson production and the W asymmetry measurements together with the HERA-I DIS charged and neutral current data. The results of this QCD analysis indicate an improvement ($\sim 5\%$ – 7%) in the gluon PDFs around the region of $x \sim 0.1$. The current analysis demonstrates the limited constraints on the gluon PDFs using inclusive Z boson data. Therefore, in order to describe the very precisely measured Z boson cross section, more accurate theoretical predictions accessible via the fast techniques to PDF fits are needed, which are expected to reduce the level of disagreement between the data and theory.

-
- [1] J. M. Campbell, J. Huston, and W. Stirling, Hard interactions of quarks and gluons: A primer for LHC physics, *Rep. Prog. Phys.* **70**, 89 (2007).
 - [2] A. Martin, W. Stirling, R. Thorne, and G. Watt, Parton distributions for the LHC, *Eur. Phys. J. C* **63**, 189 (2009).
 - [3] J. Rojo *et al.*, The PDF4LHC report on PDFs and LHC data: Results from Run I and preparation for Run II, *J. Phys. G* **42**, 103103 (2015).
 - [4] L. A. Harland-Lang, A. D. Martin, P. Motylinski, and R. S. Thorne, Parton distributions in the LHC era: MMHT 2014 PDFs, *Eur. Phys. J. C* **75**, 204 (2015).
 - [5] S. Dulat, T. J. Hou, J. Gao, M. Guzzi, J. Huston, P. Nadolsky, J. Pumplin, C. Schmidt, D. Stump, and C. P. Yuan, The CT14 Global Analysis of Quantum Chromodynamics, *Phys. Rev. D* **93**, 033006 (2016).
 - [6] J. Rojo, Progress in the NNPDF global analysis and the impact of the legacy HERA combination, *Proc. Sci.*, EPS-HEP2015 (2015) 506.
 - [7] S. Alekhin, J. Blumlein, and S. Moch, The ABM Parton Distributions Tuned to LHC Data, *Phys. Rev. D* **89**, 054028 (2014).
 - [8] G. Aad *et al.* (ATLAS Collaboration), Determination of the Strange Quark Density of the Proton from ATLAS Measurements of the $W \rightarrow \ell\nu$ and $Z \rightarrow \ell\ell$ Cross Sections, *Phys. Rev. Lett.* **109**, 012001 (2012).
 - [9] S. Chatrchyan *et al.* (CMS Collaboration), Measurement of the Muon Charge Asymmetry in Inclusive $pp \rightarrow W + X$ Production at $\sqrt{s} = 7$ TeV and an Improved Determination of Light Parton Distribution Functions, *Phys. Rev. D* **90**, 032004 (2014).
 - [10] S. Chatrchyan *et al.* (CMS Collaboration), Measurement of associated W + charm production in pp collisions at $\sqrt{s} = 7$ TeV, *J. High Energy Phys.* **02** (2014) 013.
 - [11] G. Aad *et al.* (ATLAS Collaboration), Measurement of the production of a W boson in association with a charm quark in pp collisions at $\sqrt{s} = 7$ TeV with the ATLAS detector, *J. High Energy Phys.* **05** (2014) 068.
 - [12] B. J. A. Watt, P. Motylinski, and R. S. Thorne, The effect of LHC jet data on MSTW PDFs, *Eur. Phys. J. C* **74**, 2934 (2014).
 - [13] G. Aad *et al.* (ATLAS Collaboration), Measurement of the inclusive jet cross section in pp collisions at $\sqrt{s} = 2.76$ TeV and comparison to the inclusive jet cross section at $\sqrt{s} = 7$ TeV using the ATLAS detector, *Eur. Phys. J. C* **73**, 2509 (2013).
 - [14] V. Khachatryan *et al.* (CMS Collaboration), Constraints on parton distribution functions and extraction of the strong coupling constant from the inclusive jet cross section in pp collisions at $\sqrt{s} = 7$ TeV, *Eur. Phys. J. C* **75**, 288 (2015).
 - [15] J. Rojo, Constraints on parton distributions and the strong coupling from LHC jet data, *Int. J. Mod. Phys. A* **30**, 1546005 (2015).
 - [16] M. Czakon, M. L. Mangano, A. Mitov, and J. Rojo, Constraints on the gluon PDF from top quark pair production at hadron colliders, *J. High Energy Phys.* **07** (2013) 167.
 - [17] M. Guzzi, K. Lipka, and S.-O. Moch, Top-quark pair production at hadron colliders: Differential cross section and phenomenological applications with DiffTop, *J. High Energy Phys.* **01** (2015) 082.
 - [18] CMS Collaboration, CERN Technical Report No. CMS-PAS-SMP-13-013, 2014.
 - [19] V. Khachatryan *et al.* (CMS Collaboration), Measurement of the Z boson differential cross section in transverse momentum and rapidity in proton-proton collisions at 8 TeV, *Phys. Lett. B* **749**, 187 (2015).

- [20] S. Alekhin, O. Behnke, P. Belov, S. Borroni, M. Botje *et al.*, HERAFitter, Open Source QCD Fit Project, *Eur. Phys. J. C* **75**, 304 (2015).
- [21] F. Aaron *et al.* (H1 and ZEUS Collaboration), Combined measurement and QCD analysis of the inclusive $e^\pm p$ scattering cross sections at HERA, *J. High Energy Phys.* **01** (2010) 109.
- [22] S. A. Malik and G. Watt, Ratios of W and Z cross sections at large boson p_T as a constraint on PDFs and background to new physics, *J. High Energy Phys.* **02** (2014) 025.
- [23] M. Klasen and M. Brandt, Parton Densities from LHC Vector Boson Production at Small and Large Transverse Momenta, *Phys. Rev. D* **88**, 054002 (2013).
- [24] D. V. Bandurin and N. B. Skachkov, On the possibilities of measuring the gluon distribution using gamma/Z0 + jet, events at Tevatron Run II and LHC, [arXiv:hep-ex/0403024](https://arxiv.org/abs/hep-ex/0403024).
- [25] G. Altarelli, R. K. Ellis, and G. Martinelli, Large perturbative corrections to the Drell-Yan process in QCD, *Nucl. Phys.* **B157**, 461 (1979).
- [26] G. Altarelli, R. K. Ellis, M. Greco, and G. Martinelli, Vector boson production at colliders: A theoretical reappraisal, *Nucl. Phys.* **B246**, 12 (1984).
- [27] J. C. Collins, D. E. Soper, and G. F. Sterman, Transverse momentum distribution in Drell-Yan pair and W and Z boson production, *Nucl. Phys.* **B250**, 199 (1985).
- [28] K. Melnikov and F. Petriello, Electroweak gauge boson production at hadron colliders through $O(\alpha(s)^2)$, *Phys. Rev. D* **74**, 114017 (2006).
- [29] S. Catani, L. Cieri, G. Ferrera, D. de Florian, and M. Grazzini, Vector Boson Production at Hadron Colliders: A Fully Exclusive QCD Calculation at NNLO, *Phys. Rev. Lett.* **103**, 082001 (2009).
- [30] C. Balazs and C. Yuan, Soft Gluon Effects on Lepton Pairs at Hadron Colliders, *Phys. Rev. D* **56**, 5558 (1997).
- [31] G. Ladinsky and C. Yuan, The Nonperturbative Regime in QCD Resummation for Gauge Boson Production at Hadron Colliders, *Phys. Rev. D* **50**, R4239 (1994).
- [32] R. Boughezal, J. M. Campbell, R. K. Ellis, C. Focke, W. T. Giele, X. Liu, and F. Petriello, Z-Boson Production in Association with a Jet at Next-to-Next-to-Leading Order in Perturbative QCD, *Phys. Rev. Lett.* **116**, 152001 (2016).
- [33] R. Boughezal, C. Focke, X. Liu, and F. Petriello, W-Boson Production in Association with a Jet at Next-to-Next-to-Leading Order in Perturbative QCD, *Phys. Rev. Lett.* **115**, 062002 (2015).
- [34] R. Boughezal, X. Liu, and F. Petriello, Phenomenology of the Z-Boson Plus Jet Process at NNLO, [arXiv:1602.08140](https://arxiv.org/abs/1602.08140) [*Phys. Rev. D* (to be published)].
- [35] J. R. Andersen, J. J. Medley, and J. M. Smillie, Z/γ^* plus multiple hard jets in high energy collisions, *J. High Energy Phys.* **05** (2016) 136.
- [36] T. Gehrmann, L. Tancredi, and E. Weihs, Two-loop QCD helicity amplitudes for $gg \rightarrow Zg$ and $gg \rightarrow Z\gamma$, *J. High Energy Phys.* **04** (2013) 101.
- [37] G. Aad *et al.* (ATLAS Collaboration), Measurement of the Z/γ^* boson transverse momentum distribution in pp collisions at $\sqrt{s} = 7$ TeV with the ATLAS detector, *J. High Energy Phys.* **09** (2014) 145.
- [38] Y. Li and F. Petriello, Combining QCD and Electroweak Corrections to Dilepton Production in FEWZ, *Phys. Rev. D* **86**, 094034 (2012).
- [39] J. M. Campbell and R. Ellis, MCFM for the Tevatron and the LHC, *Nucl. Phys. B, Proc. Suppl.* **205–206**, 10 (2010).
- [40] T. Carli, D. Clements, A. Cooper-Sarkar, C. Gwenlan, G. P. Salam, F. Siegert, P. Starovoitov, and M. Sutton, A posteriori inclusion of parton density functions in NLO QCD final-state calculations at hadron colliders: The APPLGRID Project, *Eur. Phys. J. C* **66**, 503 (2010).
- [41] H.-L. Lai, M. Guzzi, J. Huston, Z. Li, P. M. Nadolsky, J. Pumplin, and C.-P. Yuan, New Parton Distributions for Collider Physics, *Phys. Rev. D* **82**, 074024 (2010).
- [42] H.-L. Lai, J. Huston, Z. Li, P. Nadolsky, J. Pumplin, D. Stump, and C. P. Yuan, Uncertainty Induced by QCD Coupling in the CTEQ Global Analysis of Parton Distributions, *Phys. Rev. D* **82**, 054021 (2010).
- [43] R. D. Ball *et al.* (NNPDF Collaboration), Parton distributions for the LHC Run II, *J. High Energy Phys.* **04** (2015) 040.
- [44] R. Boughezal, X. Liu, and F. Petriello, A comparison of NNLO QCD predictions with 7 TeV ATLAS and CMS data for $V + \text{jet}$ processes, *Phys. Lett. B* **760**, 6 (2016).
- [45] V. N. Gribov and L. N. Lipatov, Deep inelastic $e p$ scattering in perturbation theory, *Yad. Fiz.* **15**, 781 (1972) [*Sov. J. Nucl. Phys.* **15**, 438 (1972)].
- [46] L. N. Lipatov, The parton model and perturbation theory, *Yad. Fiz.* **20**, 181 (1974) [*Sov. J. Nucl. Phys.* **20**, 94 (1975)].
- [47] G. Altarelli and G. Parisi, Asymptotic freedom in parton language, *Nucl. Phys.* **B126**, 298 (1977).
- [48] Y. L. Dokshitzer, Calculation of the structure functions for deep inelastic scattering and e^+e^- annihilation by perturbation theory in quantum chromodynamics, *Zh. Eksp. Teor. Fiz.* **73**, 1216 (1977) [*Sov. Phys. JETP* **46**, 641 (1977)].
- [49] M. Botje, QCDNUM: Fast QCD evolution and convolution, *Comput. Phys. Commun.* **182**, 490 (2011).
- [50] R. Thorne, A Variable-Flavor Number Scheme for NNLO, *Phys. Rev. D* **73**, 054019 (2006).